ChemComm

Accepted Manuscript

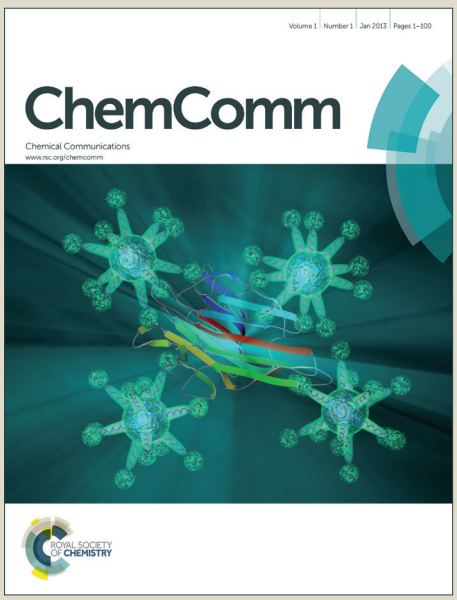

ROYAL SOCIETY OF CHEMISTRY

www.rsc.org/chemcomm

Journal Name

RSCPublishing

COMMUNICATION

Co Intake Mediated Formation of Ultrathin Nanosheets of Transition Metal LDH — an Advanced Electrocatalyst for Oxygen Evolution Reaction

Cite this: DOI: 10.1039/x0xx00000x

Received 00th January 2012,
Accepted 00th January 2012

DOI: 10.1039/x0xx00000x

www.rsc.org/

Xia Long [a], Shuang Xiao [a], Zilong Wang [a], Xiaoli Zheng [a], and Shihe Yang [a]*

By controlling the ratio of tri- and bi-valent ions, multi-transition metals based layered double hydroxide (LDH) ultrathin nanosheets are synthesized. They show advanced OER performance with low overpotentials (~0.2 V) and decreased Tafel slopes with increasing Co incorporation due to the modulated electronic structures of catalytic centers and the increased surface area and electronic conductivity.

Water splitting to form H_2 and O_2, which would enable large scale storage of intermediate energy from renewable sources, has aroused intense studies recently. However, the energy efficiency of water splitting is significantly lost due to the slow kinetics of oxygen revolution reaction (OER). Therefore, an effective and stable catalyst to reduce the large overpotential and accelerate the OER reaction is highly required. Noble metal oxides such as IrO_2 and RuO_2 exhibit the best OER activity,[1] but the elemental scarcity and high cost have greatly hindered their widespread applications. Therefore, exploring earth abundant element based catalysts without compromising the high catalytic performances for OER is still a great challenge.

Recently, first low transition metal oxides and hydroxides have been under intensive scrutiny as low cost catalysts for renewable energy applications.[2] It has been found that the OER active materials are layered hydroxides or oxyhydroxides composed of edge sharing octahedral MO_6 layers,[2h, 3] and their activity could be further improved after the exfoliation process.[3a, 4] Meanwhile, many studies found that mixed metal hydroxides/oxides exhibit higher catalytic performance than their monary counterparts,[2g, 4a, 5] possibly related to the changed electronic structure[2f, 6] or the enhanced electrical conductivity[6a] of the catalyst with the incorporation of "impurities". However, the precise roles of the primary transition metals as well as the "impurities" in improving the OER activity of catalysts still have not been unravelled.

In this work, without any further exfoliation treatments, bi-(FeNi) and tri-mental (Fe, Ni and Co) LDH with controlled Co incorporations and atomic thickness were successfully obtained by a one step hydrothermal method (see Scheme S1), which showed advanced OER activity with overpotential as low as 0.21 V and Tafel slopes ranging from 55 mV/dec to 42 mV/dec that decreased with increasing Co content. Besides the increased specific surface area with the increased Co incorporation, it was revealed that the increased number of the active sites, improved electronic conductivity as well as enhanced activity of the catalytic sites brought by the minor "impurities" (Fe and Co) also contributed to the superior electrochemical catalytic performances of the FeNiCo LDH ultrathin nanosheets towards OER.

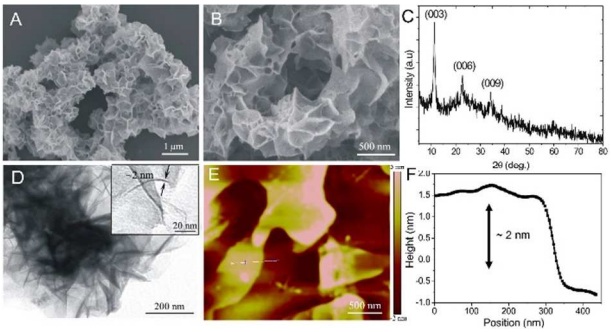

Figure 1. SEM (A, B) images, XRD pattern (C), TEM image (D), AFM height image (E) and corresponding height as a function of position curve (F) of FeNi LDH nanosheets. Inset images in D is the enlarged TEM image of standing nanosheets showing the thickness of LDH.

FeNi LDH, which was reported to be an OER active material,[3a, 4] was synthesized via a hydrothermal method (see SI for detail). By precisely tuning the ratios of Fe^{3+} to Ni^{2+} in the mother solution, the as-formed product changed from $Ni(OH)_2$ in microscale to FeNi LDH in nanoscale (Figure S1). After exploring a variety of parameters, Fe/Ni=1/10 was identified as the best ratio for forming the ideal product. The scanning electron microscopy (SEM, Figure 1A, B) and transmission electron microscopy (TEM, Figure 1D, S2A) images show that they are nanosheets. The energy dispersive X-ray spectroscopy (EDX) mapping (Figure S3) revealed the uniform distribution of Fe and Ni in the formed nanosheets with Fe/Ni ratios to be 1/10, consistent with the X-ray photoelectron spectra (XPS) result (Figure S4). From the standing LDH nanosheet, the thickness of $FeNi_{10}$ LDH was measured to be ~2 nm (Figure 1D inset), which was further confirmed by the atomic force microscopy (AFM) height imaging (Figure 1E, F).

XRD spectrum (Figure 1C) showed the characteristic diffraction peaks at 11.28 º, 22.76 º, and 34.14 º, which could be well indexed to the (003), (006) and (009) planes of LDHs. In addition, the high-resolution TEM (HRTEM) image of a selected nanosheet shows lattice fringes of (012) planes with a d spacing of 0.19 nm (Figure S2B). The basal spacing was calculated to be 0.78 nm along the *c* axis from the peak position of (003) plane, indicating that the ultrathin nanosheets composed of two octahedral $M(OH)_6$ layers.

Considering the high catalytic activity of Co towards OER, FeNiCo LDHs with tuneable Co contents were synthesized by precisely controlling the amount of added cobalt salt in the mother solution. The SEM (Figure S5A, D) and TEM (Figure S5B, E) images of these LDHs revealed that they are in platelet like structures akin to that of $FeNi_{10}$ LDH (Figure 1). EDX mapping (Figure S6) showed the uniform distribution Fe, Ni and Co in the nanosheets. XPS spectra showed the intensity of Co increased with the increase of Co addition in mother solution (Figure S7). Moreover, both the EDS and XPS results suggested that the Fe/Ni/Co ratios of synthesized LDHs were 1/9/1 and 1/8/2, respectively, which were in good agreement with the corresponding solution stoichiometries. The XRD of FeNiCo LDHs (Figure S8) showed that only (003) diffraction peak remains pronounced whereas the (006) and (009) peaks become ambiguous due most likely to the ultrathin structure of the LDHs (only about two layers). This is consistent to the report of Hu et al, who showed that the (00n) diffraction peaks disappear once the bulk LDH is exfoliated into single layers.[3a] Moreover, the (003) diffraction peak is positively shifted with the Co incorporation (Figure S8B) from 11.28º for $FeNi_{10}$ LDH to 11.45º and 12.9º for $FeNi_9Co$ LDH and $FeNi_8Co_2$ LDH, respectively, suggesting a decrease in d-spacing along the *c* axis from 0.78 nm to 0.77 nm and 0.68 nm due to the substitution of Ni^{2+} with Co^{2+}. Indeed, the TEM images (insets in Figure S5B, E) and the AFM height images (Figure S5C, F) show that with the increase of Co content, the thickness of LDHs decreases, namely from ~2 nm for $FeNi_{10}$ LDH (Figure 1D-F) to 1.5~1.8 nm for $FeNi_9Co$ LDH (Figure S5C), and to 1.2 ~ 1.5 nm for $FeNi_8Co_2$ LDH (Figure S5F). To our knowledge, this is the first time that such FeNiCo LDH ultrathin nanosheets with tuneable FeNiCo ratios and thicknesses smaller than 2 nm are prepared.

Transition metal based ultrathin nanosheets with single or few atomic layers, are expected to have high surface activity and rich electronic properties that may render intriguing applications in energy storage and conversion.[7] Herein, the as-synthesized ultrathin FeNi and FeNiCo LDH nanosheets were investigated as electrochemical catalyst towards OER in a typical three-electrode configuration in 1 M KOH. Firstly, the FeNiCo LDHs were deposited onto Ni foam for cyclic voltammetry (CV) (Figure S9) measurements. We observed redox current peaks at around 1.38 V, which correspond to the reversible reactions of Ni(II)/Ni(III or IV)[4a] for all the LDH samples. Moreover, the current density spiked at around 1.44 V, signalling the onset of water splitting. Further, linear sweep voltammetry (LSV) tests were used to investigate the catalytic activities of the set of OER catalysts after 95% iR-correction (Figure 2A). Consistent to the CV results, the current density of catalyzed OER spiked around 1.44 V. The overpotentials of these FeNi and FeNiCo LDHs catalyzed OER are close to each other, suggesting that they have similar catalytic centres. Moreover, the low overpotential of 0.21 V indicates that they are among the most active non-noble metal based electrochemical catalyst for OER.[4b, 5a, 8] Further, the FeNiCo LDH ultrathin nanosheets were loaded on glass carbon as working electrode. The LSV curves of OER (Figure S10A) confirmed the low onset potential of ~0.21 V, in agreement with the results obtained on the Ni foam electrodes. However, the current density of OER on GC electrode was smaller than that on Ni foam electrode at the same applied voltage (Figure S10B), due plausibly to the three-dimensional structure of Ni foam with a larger surface area. Apart from the intrinsically high catalytic activity of the transition metals used, the ultrathin nanosheet structure might also be important to the advanced catalytic performance of LDHs. First, layered hydroxides or oxyhydroxides composed of edge sharing octahedral MO_6 layers were reported to be OER active, as observed in a NiOOH material *in situ* transformed from NiO,[2h] and further revealed in both amorphous Co-phosphate and Ni-borate catalysts and crystalline metal oxides.[3] Second, the layered structure is relatively open, thus permits fast diffusion of reactants or products and rapid proton-coupled electron transfer and allows the catalytic active sites easily accessible,[9] giving rise to the high electrocatalytic activity toward OER.[8b, 10] Moreover, the atomic thickness endows FeNi and FeNiCo LDH ultrathin nanosheets with improved surface activity than their bulk materials that further increased their OER performances.

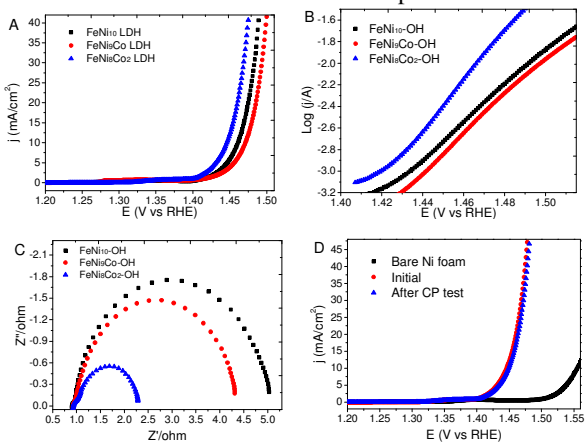

Figure 2. Electrocatalytic OER performance of the FeNiCo LDH nanosheets. (A) Linear sweep voltammetry polarization curves. (B) Tafel plots. (C) Electrochemical impendence of FeNiCo LDH with different Fe/Ni/Co ratios at overpotential of 0.3 V. (D) LSV curves of bare Ni foam, $FeNi_8Co_2$ LDH before and after chronopotentiometry test for 11 hours. Catalyst loading was ~0.25 mg/cm^2.

The potentials required to achieve the current density of 10 mA/cm^2, which is the approximately current density for a 10% efficient solar-to-fuel conversion device,[5a, 11] decreased with the increase of the Co incorporation (1.472V, 1.462 V, and 1.45 V for $FeNi_{10}$, $FeNi_9Co$, and $FeNi_8Co_2$ LDH, respectively), indicating a higher catalytic performance of FeNiCo LDH nanosheets with higher Co contents. N_2 adsorption-desorption isotherms (Figure S11) show that the specific surface area of $FeNi_{10}$ LDH, $FeNi_9Co$ LDH, and $FeNi_8Co_2$ LDH were 46.05 m^2/g, 54.18 m^2/g and 80.44 m^2/g, respectively, which increased with the increase of Co incorporation and might lead to more exposed catalytic active sites.

Tafel slope describes the influence of potential on the steady-state current density and is an important factor for evaluating OER kinetics. The estimated Tafel slopes of the as-synthesized LDHs are 55 mV/dec, 52 mV/dec, and 42 mV/dec for $FeNi_{10}$ LDH, $FeNi_9Co$ LDH, and $FeNi_8Co_2$ LDH, respectively (Figure 2B), which decreased with the increase of Co doping. It is worth noting that the value of $FeNi_8Co_2$ LDH catalyzed OER is close to that of the well-established OER catalysts of IrO_2 (~49 mV /dec)[2h, 12] as well as exfoliated LDH nanosheets (45, 41,

and 40 mV/dec for CoCo, NiCo, and NiFe LDH nanosheets, respectively),[3a] indicating an efficient electrocatalytic activity of synthesized FeNiCo LDH ultrathin nanosheets.

It is known that the high conductivity of catalysts would facilitate the charge transport, minimize the potential drop, and thus lead to good catalytic activities. Early in 1987, Corrigan et al.[6a] found that the OER activity of $Ni(OH)_2$ was enhanced with Fe doping and an increased conductivity was hypothesized to be the critical factor. Recently, by studying the conductivity of $Ni_{1-x}Fe_xOOH$ as a function of Fe content, Boettcher et al.[5b] confirmed that electronic conductivity of $Ni_{1-x}Fe_xOOH$ film increased with Fe addition. In this work, the conductivities of both FeNi and FeNiCo LDH nanosheets were measured by electrochemical impendence spectroscopy (EIS, Figure 2C). The semicircle diameter in the high frequency range of the Nyquist plot is associated with the charge transfer resistance (R_{ct}) and a low R_{ct} value corresponds to a fast reaction rate.[13] From Figure 2C, one can see that the R_{ct} values of the LDHs decrease with increasing Co incorporation at the potential of 1.48 V, indicating an enhanced OER activity of FeNiCo LDHs, concurring with the results of Tafel plots (Figure 2B). The low charge transfer resistance, which benefits the efficient charge transport, is partly due to the decreased thickness of LDH nanosheets, on top of the synergistic effect stemming from the multiple transition metals present, as well as other intrinsic factors, e.g., the dopant role of the Co in a way similar to Fe as a dopant to improve the conductivity of titanium.[14]

Next, assuming that all of the metal ions in the catalysts were involved in the electrochemical reaction, the OER turnover frequencies (TOFs) at the overpotential of 0.3 V were calculated. It should be pointed out that the as-calculated TOFs could be gross underestimations of the actual TOFs because not every metal atom is catalytically active. Nevertheless, even with these overly conservative estimations, the TOFs are still respectable: 0.53 s^{-1} for $FeNi_{10}$ LDHs, 0.55 s^{-1} for $FeNi_9Co$ LDHs and 0.7 s^{-1} for $FeNi_8Co_2$ LDHs, all higher than previously reported values under comparable measurement conditions. [2h, 4b, 5a, 8b]

As the most active OER catalyst, the $FeNi_8Co_2$ LDH nanosheets were investigated for assessing their stability. It outperformed the reported earth abundant metal hydroxide OER catalysts[4b, 5a] at high current densities, such as 5 mA/cm^2, 10 mA/cm^2, and 20 mA/cm^2, by low required potentials at 1.441 V, 1.454 V, and 1.469 V, respectively (Figure S12). The high current density is ascribed to the high activity of the catalyst, because the bare Ni foam exhibited little current density under the potential lower than 1.5 V (Figure 2D, black curve). Moreover, the potential required to achieve the current density of 10 mA/cm^2 was kept nearly unchanged during the chronopotentiometry (CP) measurement for 11 hours (Figure S13), whereas for the RuO_2 catalyst, the required potential showed an increase with the measurement time. Consistently, a similar LSV curve with nearly the same onset potential after the CP test was recorded (Figure 2D, blue curve), indicating the superior stability and durability of the FeNiCo LDH catalysts.

Raman spectra (Figure 3) of the FeNiCo LDHs were collected to further correlate the structure of FeNiCo LDH with the chemical composition as well as the electrochemical performance of the catalysts. From the deconvoluted Raman spectra, the band around 460 cm^{-1} (red fitted curves) is attributed to the Ni-O vibration of β-$Ni(OH)_2$ (~450 cm^{-1}). The positive shift of this band could be ascribed to the incorporation of Co and Fe as reported previously.[6b] The bands centred at 474 cm^{-1} and 555 cm^{-1} (blue fitted curves) are assigned to the Ni-O vibration in NiOOH,[6b, 15] which was reported to be the direct OER active mediator.[2h] Moreover, the relative intensities of Ni-O bands varied with the incorporation of cobalt, indicating a change in the local environment of Ni-O. In addition, the green fitted curve centred at 500 cm^{-1} (Figure 3C, D) from the deconvolution of the Raman spectra of the Co incorporated LDHs ($FeNi_9Co$ LDH and $FeNi_8Co_2$ LDH) indicates the identity of the Co-O band in CoOOH.[16] It was reported previously that the incorporation of cobalt could improve the electronic conductivity of the catalyst. Moreover, CoOOH is able to enhance the electron transport as well as the proton migration through the nickel hydroxide electrode,[17] and can thus increase the electrode utilization and electrochemical performance of the LDH nanosheets. Therefore, besides the increased active sites of FeNiCo LDH resulting from the increased specific surface area and reduced electron transfer resistance due to the incorporation of Co, the increased activity of the Ni sites brought about by the Fe and Co neighbours, is also proposed to be a fundamental factor responsible for the enhanced OER electrochemical performance of the FeNiCo LDH nanosheets.

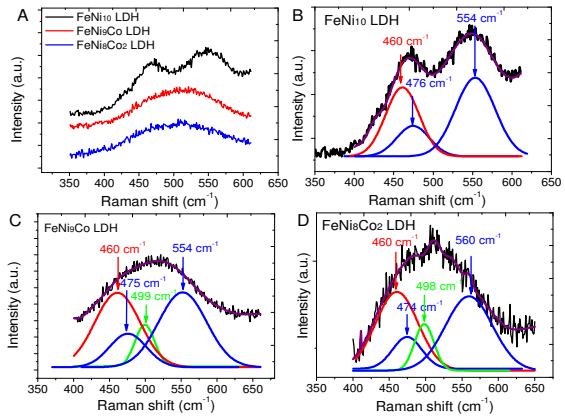

Figure 3. Raman spectra of $FeNi_{10-x}Co_x$ (x=0~3) LDHs. (A) Ni-O bands of FeNiCo LDHs, (B) deconvoluted Ni-O Raman spectra of $FeNi_{10}$ LDH, (C) deconvoluted Ni-O Raman spectra of $FeNi_9Co$ LDH, (D) deconvoluted Ni-O Raman spectra of $FeNi_8Co_2$ LDH. Red fitted curve: Ni-O band of β-$Ni(OH)_2$, which should be around 450 cm^{-1}; blue fitted curves: Ni-O band of NiOOH at 474 cm^{-1} and 554 cm^{-1}; green fitted curve: Co-O band of CoOOH at 500 cm^{-1}.

In general, the activities of transition metal based OER catalysts are thought to relate to the 3d electron number of transition metal ions, the enthalpy for the lower to higher oxide transition, and the surface oxygen binding energy.[12,18] Moreover, the e_g orbital of surface transition metal ions could bond with anion adsorbates[18d] and thus influence the binding of oxygenic intermediate species and thus the OER activity.[19] Take $FeNi_8Co_2$ LDH as a typical example, XPS analysis was conducted (Figure S14) to better understand the oxidation state of catalytic metal ions. In the O 1s region, the spectra of $FeNi_8Co_2$ LDH could be deconvoluted to four oxygen peaks, which correspond to Fe-O (531.4 eV), Ni-O (531.7 eV), Co-O (532.7 eV), [20] and physi- and chemi-sorbed water at or near the surface (533.9 eV).[20a, 20b, 21] The Co 2p feature of $FeNi_8Co_2$ LDH (Figure S14B) was best fitted with two shakeup satellites (yellow curves), and two spin-orbit doublets, characteristic of Co^{2+} (blue curve) and Co^{3+} (green curve).[22] The electronic configurations of Co^{2+} and Co^{3+} were most likely $t_{2g}^6e_g^1$ and $t_{2g}^5e_g^1$, respectively. In the Ni 2p region of $FeNi_8Co_2$ LDH (Figure S14C), the binding energy of Ni peaks were positively shifted, suggesting the strong interactions involving Ni and

Co.[20c] Moreover, besides the three shakeup satellites (yellow curves) and the Ni^{2+} peak (blue curves), a Ni^{3+} feature (green curves) associated with the electronic configuration of $t_{2g}^{6}e_{g}^{1}$ could also be deconvoluted,[20a, 20b] which may account for the improved OER activity. This is consistent with the result of Suntvich et al. that the intrinsic OER activity has a volcano-shaped dependence on the 3d-occupancy of the transition metal cations, peaking at an e_g occupancy close to unity.

In conclusion, transition metal LDH ultrathin nanosheets with tuneable chemical compositions have been successfully synthesized. The as-prepared LDHs showed advanced electrocatalytic performances on OER with overpotentials as low as 0.21 V and Tafel slopes down to 42 mV/dec. The high catalytic activity of these LDHs outperform most of earth abundant OER catalysts reported thus far[5a, 8b] and are comparable to that of noble metal catalysts[2h, 4b, 12, 23] as well as exfoliated LDH[3a] (Table S1). Moreover, the catalytic kinetics of as synthesized FeNiCo LDH increased with the increase of Co incorporation, which was revealed to be resulted from the increased specific surface that supplied more catalytic active sites, reduced charge transference resistance and improved activity of catalytic center arising from the modulated electronic structure. This work shed light on the effects of cobalt in the performance of transition metals based electrocatalysts and also important for comparison with theoretical predictions and ultimately a complete understanding of the origin of high activity in FeNiCo based OER electrocatalysts, which would be beneficial to develop new strategies to design low cost electrocatalysts toward OER.

Notes and references

[a] Department of Chemistry, William Mong Institute of Nano Science and Technology, The Hong Kong University of Science and Technology, Clear Water Bay, Kowloon, Hong Kong

* Corresponding author: chsyang@ust.hk

Electronic Supplementary Information (ESI) available: Experimental details, SEM, TEM, EDX, BET, XRD, XPS and CP of catalysts. See DOI: 10.1039/c000000x/

Acknowledgement: This work was supported by the HK-RGC General Research Funds (HKUST 606511 and 605710).

[1] D. Galizzioli, F. Tantardini, S. Trasatti, *J. Appl. Electrochem.* **1974**, *4*, 57-67.

[2] a) S. Chen, J. Duan, W. Han, S. Z. Qiao, *Chem. Commun.* **2014**, *50*, 207-209; b) J. A. Haber, C. Xiang, D. Guevarra, S. Jung, J. Jin, J. M. Gregoire, *ChemElectroChem* **2013**, *1*, 524-528; c) T. W. Kim, K.-S. Choi, *Science* **2014**, *343*, 990-994; d) A. Kleiman-Shwarsctein, Y.-S. Hu, G. D. Stucky, E. W. McFarland, *Electrochem. Commun.* **2009**, *11*, 1150-1153; e) M. D. Merrill, R. C. Dougherty, *J. Phys. Chem. C* **2008**, *112*, 3655-3666; f) R. D. Smith, M. S. Prévot, R. D. Fagan, S. Trudel, C. P. Berlinguette, *J. Am. Chem. Soc.* **2013**, *135*, 11580-11586; g) R. D. Smith, M. S. Prévot, R. D. Fagan, Z. Zhang, P. A. Sedach, M. K. J. Siu, S. Trudel, C. P. Berlinguette, *Science* **2013**, *340*, 60-63; h) L. Trotochaud, J. K. Ranney, K. N. Williams, S. W. Boettcher, *J. Am. Chem. Soc.* **2012**, *134*, 17253-17261; i) X. Zou, X. Huang, A. Goswami, R. Silva, B. R. Sathe, E. Mikmeková, T. Asefa, *Angew. Chem.* **2014**, *126*, 4461-4465; j) K. Fominykh, J. M. Feckl, J. Sicklinger, M. Döblinger, S. Böcklein, J. Ziegler, L. Peter, J. Rathousky, E. W. Scheidt, T. Bein, *Adv. Funct. Mater.* **2014**, *24*, 3123-3129.

[3] a) F. Song, X. Hu, *Nat. Commun.* **2014**, *5*; b) Y. Surendranath, D. A. Lutterman, Y. Liu, D. G. Nocera, *J. Am. Chem. Soc.* **2012**, *134*, 6326-6336; c) D. K. Bediako, B. Lassalle-Kaiser, Y. Surendranath, J. Yano, V. K. Yachandra, D. G. Nocera, *J. Am. Chem. Soc.* **2012**, *134*, 6801-6809; d) R. L. Doyle, I. J. Godwin, M. P. Brandon, M. E. Lyons, *Phy. Chem. Chem. Phy.* **2013**, *15*, 13737-13783; e) I. Godwin, M. Lyons, *Electrochem. Commun.* **2013**, *32*, 39-42.

[4] a) X. Long, J. Li, S. Xiao, K. Yan, Z. Wang, H. Chen, S. Yang, *Angew. Chem. Int. Edit.* **2014**, *53*, 7584-7588; b) M. Gong, Y. Li, H. Wang, Y. Liang, J. Z. Wu, J. Zhou, J. Wang, T. Regier, F. Wei, H. Dai, *J. Am. Chem. Soc.* **2013**, *135*, 8452-8455.

[5] a) C. C. McCrory, S. Jung, J. C. Peters, T. F. Jaramillo, *J. Am. Chem. Soc.* **2013**, *135*, 16977-16987; b) L. Trotochaud, S. L. Young, J. K. Ranney, S. W. Boettcher, *J. Am. Chem. Soc.* **2014**, *136*, 6744-6753; c) T. Alexis, *Energ. Environ. Sci.* **2014**, *7*, 682-688; d) C. Xiang, S. K. Suram, J. A. Haber, D. W. Guevarra, J. Jin, J. M. Gregoire, *ACS Comb. Sci.* **2013**, *16*, 47-52; e) J. B. Gerken, J. Y. Chen, R. C. Massé, A. B. Powell, S. S. Stahl, *Angew. Chem. Int. Edit.* **2012**, *51*, 6676-6680; f) J. B. Gerken, S. E. Shaner, R. C. Masse, N. J. Porubsky, S. Stahl, *Energ. Environ. Sci.* **2014**, *7*, 2376-2382.

[6] a) D. A. Corrigan, *J. Electrochem. Soc.* **1987**, *134*, 377-384; b) M. W. Louie, A. T. Bell, *J. Am. Chem. Soc.* **2013**, *135*, 12329-12337.

[7] a) J. Feng, X. Sun, C. Wu, L. Peng, C. Lin, S. Hu, J. Yang, Y. Xie, *J. Am. Chem. Soc.* **2011**, *133*, 17832-17838; b) C. Wu, X. Lu, L. Peng, K. Xu, X. Peng, J. Huang, G. Yu, Y. Xie, *Nat. Commun.* **2013**, *4*, 2431; c) L. Cheng, W. Huang, Q. Gong, C. Liu, Z. Liu, Y. Li, H. Dai, *Angew. Chem. Int. Edit.* **2014**, *53*, 7860-7863; d) S. Jin, M. A. Lukowski, A. S. Daniel, C. R. English, F. Meng, A. Forticaux, R. Hamers, *Energ. Environ. Sci.* **2014**, *7*, 2608-2613.

[8] a) J. Landon, E. Demeter, N. İnoğlu, C. Keturakis, I. E. Wachs, R. Vasić, A. I. Frenkel, J. R. Kitchin, *ACS Catalysis* **2012**, *2*, 1793-1801; b) X. Zou, A. Goswami, T. Asefa, *J. Am. Chem. Soc.* **2013**, *135*, 17242-17245.

[9] a) Q. Yin, J. M. Tan, C. Besson, Y. V. Geletii, D. G. Musaev, A. E. Kuznetsov, Z. Luo, K. I. Hardcastle, C. L. Hill, *Science* **2010**, *328*, 342-345; b) B. S. Yeo, A. T. Bell, *J. Am. Chem. Soc.* **2011**, *133*, 5587-5593; c) Y. Surendranath, M. W. Kanan, D. G. Nocera, *J. Am. Chem. Soc.* **2010**, *132*, 16501-16509; d) J. B. Gerken, J. G. McAlpin, J. Y. Chen, M. L. Rigsby, W. H. Casey, R. D. Britt, S. S. Stahl, *J. Am. Chem. Soc.* **2011**, *133*, 14431-14442.

[10] M. Wehrens-Dijksma, P. Notten, *Electrochim. Acta* **2006**, *51*, 3609-3621.

[11] M. G. Walter, E. L. Warren, J. R. McKone, S. W. Boettcher, Q. Mi, E. A. Santori, N. S. Lewis, *Chem. Rev.* **2010**, *110*, 6446-6473.

[12] S. Trasatti, *J. Electroanal. Chem.* **1980**, *111*, 125-131.

[13] a) D. Merki, H. Vrubel, L. Rovelli, S. Fierro, X. Hu, *Chem. Sci.* **2012**, *3*, 2515-2525; b) T. Wang, L. Liu, Z. Zhu, P. Papakonstantinou, J. Hu, H. Liu, M. Li,*Energy Environ. Sci.*, **2013**, *6*, 625–633; c) Z. Lu, W. Xu, W. Zhu, Q. Yang, X. Lei, J.Liu, Y. Li, X. Sun, X. Duan, *Chem. Commun.***2014**, 50, 6479–6482.

[14] B. Danzfuss, U. Stimming, *J. Electroanal. Chem.* **1984**, *164*, 89-119.

[15] a) R. Kostecki, F. McLarnon, *J. Electrochem. Soc.* **1997**, *144*, 485-493; b) S. I. C. de Torresi, K. Provazi, M. Malta, R. M. Torresi, *J. Electrochem. Soc.* **2001**, *148*, A1179-A1184.

[16] T. Pauporté, L. Mendoza, M. Cassir, M. Bernard, J. Chivot, *J. Electrochem. Soc.* **2005**, *152*, C49-C53.

[17] A. Audemer, A. Delahaye, R. Farhi, N. Sac-Epée, J.-M. Tarascon, *J. Electrochem. Soc.* **1997**, *144*, 2614-2620.

[18] a) J. Rossmeisl, Z. W. Qu, H. Zhu, G. J. Kroes, J. K. Norskov, *J. Electroanal. Chem.* **2007**, *607*, 83-89; b) I. C. Man, H. Y. Su, F. Calle-Vallejo, H. A. Hansen, J. I. Martinez, N. G. Inoglu, J. Kitchin, T. F. Jaramillo, J. K. Norskov, J. Rossmeisl, *ChemCatChem* **2011**, *3*, 1159-1165; c) J. O. Bockris, T. Otagawa, *J. Electrochem. Soc.* **1984**, *131*, 290-302; d) T. A. Betley, Q. Wu, T. Van Voorhis, D. G. Nocera, *Inorg. chem.* **2008**, *47*, 1849-1861.

[19] J. Suntivich, K. J. May, H. A. Gasteiger, J. B. Goodenough, Y. Shao-Horn, *Science* **2011**, *334*, 1383-1385.

[20] a) C. Shang, S. Dong, S. Wang, D. Xiao, P. Han, X. Wang, L. Gu, G. Cui, *ACS Nano* **2013**, *7*, 5430-5436; b) C. Yuan, J. Li, L. Hou, X. Zhang, L. Shen, X. W. D. Lou, *Adv. Funct. Mater.* **2012**, *22*, 4592-4597; c) Z. Zhao, H. Wu, H. He, X. Xu, Y. Jin, *Adv. Funct. Mater.* **2014**.

[21] J. Marco, J. Gancedo, M. Gracia, J. Gautier, E. Rıos, F. Berry, *J. Solid State Chem.* **2000**, *153*, 74-81.

[22] L. Shen, Q. Che, H. Li, X. Zhang, *Adv. Funct. Mater.* **2014**, *24*, 2630-2637.

[23] S. Trasatti, G. Lodi, *Electrodes of conductive metallic oxides*, Elsevier Amsterdam, **1981**.

